ELSEVIER

Journal of Molecular Structure: THEOCHEM 856 (2008) 105–111

THEO CHEM

www.elsevier.com/locate/theochem

Computational study on dipole moment, polarizability and second hyperpolarizability of nitronaphthalenes

Vito Librando *, Andrea Alparone, Zelica Minniti

Research Centre for Analysis, Monitoring and Minimization Methods of Environmental Risk, Department of Chemistry, University of Catania, viale A. Doria 8, Catania 95125, Italy

Received 6 August 2007; received in revised form 14 January 2008; accepted 19 January 2008
Available online 1 February 2008

Abstract

Geometries, dipole moments, polarizabilities and second-order hyperpolarizabilities of nitronaphthalene (NN) isomers and of structurally related reference compound nitrobenzene were studied using conventional ab initio (HF, MP2) and density functional theory (B3LYP, PBE0) methods in conjunction with cc-pVDZ, aug-cc-pVDZ, 6-31G* and 6-31+G* basis sets. Dynamic (hyper)polarizabilities were determined through the time-dependent-HF theory at the HF/6-31+G* level at the experimental laser radiation energies of 0.02385, 0.03457 and 0.04282 a.u. Vibrational contributions to the (hyper)polarizabilities were obtained within the double harmonic approximation. Nitronaphthalenes are prototypes of nitro-polycyclic aromatic hydrocarbons (NPAHs), potentially mutagenic environmental pollutants. Different pathways have been proposed to explain mutagenic activation of NPAHs, which mainly involve penetration and diffusion in the cell, intermolecular interactions with the active site of enzymes, reduction and/or oxidation reactions. Present calculations indicate that all the electric properties increase concordantly on passing from 1-NN to 2-NN isomer due to a stronger π-conjugative interaction between the nitro group and the aromatic system. These results are consistent with the mutagenic potency of these nitroaromatics, which upon going from 1-NN to 2-NN isomer increases by 2–4 times, suggesting that binding affinity to enzymes might be a critical step in the mechanisms of metabolic mutagenic activation.

Keywords: Nitronaphthalenes; Density functional theory; Mutagenic activity; Dipole moment; (Hyper)polarizabilities

1. Introduction

Nitro-polycyclic aromatic hydrocarbons (NPAHs) have received great attention since are considered among the most potent mutagenic and carcinogenic environmental contaminants [1,2]. They are mainly produced from combustion processes and reactions between polycyclic aromatic hydrocarbons and NO_x and are also present in the food chain [1,2]. In pursuing remediation of these recalcitrant species from polluted sites, beside traditional methodologies, new approaches using biodegradative microorganism are gaining ground [3,4]. Nitronaphthalene (NN) is the smallest NPAH and exists in two isomers, 1-NN and 2-NN. Hitherto, experimental structure of NN isomers is unknown. At AM1 [5], PM3 [6] and B3LYP/6-31G* [7] levels of theory 1-NN exhibits O–N–C–C dihedral angle of 60°, 28° and 25°, respectively, whereas 2-NN isomer is planar. There are indications showing that, mutagenic potency of NPAHs is ruled by the planarity between nitro substituents and aromatic system [8]. Generally, planar or quasi-planar NPAHs exhibit mutagenic potencies higher than those of less planar isomers [8]. In the specific case of NNs mutagenic activity of 2-NN estimated according to the Ames test is about 2–4 times greater than that for 1-NN isomer [9,10]. Proposed metabolic mechanisms of NPAHs involve transport and diffusion in the cellular system, binding to enzymes, reduction and/or oxidation reactions [11]. Mutagenic activity of NPAHs has been often related to nitroreductive properties, which can be estimated by half-wave reduction potential, electron affinity (EA) or LUMO eigenvalue [1,2,7,11]. However experimental EA values of NN isomers are close to each other [12] and reductive

* Corresponding author.
E-mail address: vlibrando@unict.it (V. Librando).

0166-1280/$ - see front matter © 2008 Elsevier B.V. All rights reserved.
doi:10.1016/j.theochem.2008.01.022

mechanisms cannot elucidate their different mutagenic behavior. In alternative, metabolic pathways to mutagenic activation might be governed by binding affinity between NPAHs and the active site of enzymes [11]. Intermolecular interactions are controlled by electrostatic, inductive and dispersive effects, which depend on permanent and induced electronic charge distributions. Dipole and quadrupole moments as well as electronic (hyper)polarizabilities have been employed to understand binding affinity in enzyme–substrate complexes [13–19].

In this work we computed dipole moment (μ), electronic polarizability (α) and second hyperpolarizability (γ) of NN isomers in order to explore the effect of the nitro group substitution on these properties and elucidate the effect of the structure on the mutagenic activities. To this purpose, conventional ab initio SCF-MO and density functional theory (DFT) methods were employed. Calculations were also performed on reference compound NB, for which some experimental estimates are available in the literature.

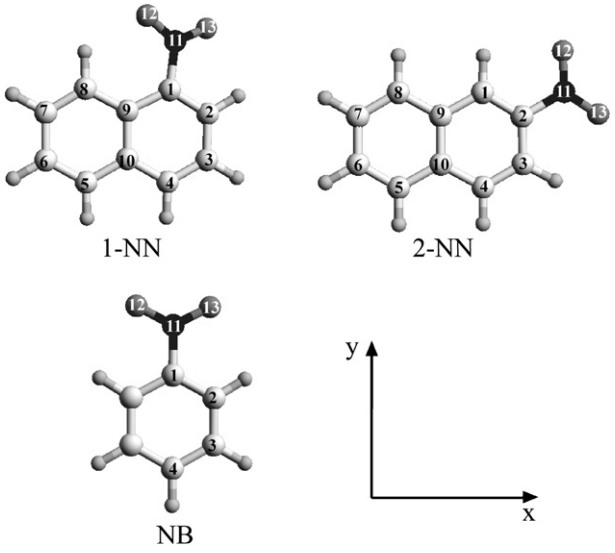

Fig. 1. Structure, atomic numbering and Cartesian coordinate system of the investigated compounds.

2. Computational methods

Geometry on NN isomers (see Fig. 1) was fully optimized by DFT-B3LYP [20,21] method in conjunction with cc-pVDZ basis set [22]. Dipole moments and static electronic (hyper)polarizabilities were calculated by HF, MP2 and DFT-PBE0 [23] methods with 6-31G* [24], 6-31+G* [24] and aug-cc-pVDZ basis sets [22]. It is important to point out that 6-31+G* basis set was previously used for (hyper)polarizability computations on π-conjugated molecules, giving results comparable to those obtained with much more extended 6-311+G(d), 6-311++G(d,p), 6-311++G(2d,2p), 6-311++G(2df,2pd), 6-311++G(3df,3pd) basis sets [25]. Correlated static electronic (hyper)polarizability values were obtained through a finite-field (FF) procedure described in detail in Ref. [26], using a field strength of 0.003 a.u.. Accuracy of finite-field computations was verified by comparing numerical μ_i, $\alpha^e{}_{ii}$ and $\gamma^e{}_{iijj}$ component values with those obtained analytically by means of the time-dependent-HF (TD-HF) theory [27,28]. Frequency-dependent electronic $\alpha^e{}_{ii}$ and $\gamma^e{}_{iijj}$ values were obtained by means of TD-HF approach at the HF/6-31+G level of calculation at the experimental laser radiation energies ($\hbar\omega$) of 0.02385, 0.03457 and 0.04282 a.u. For γ^e the usual non linear optical (NLO) phenomena were explored: Third Harmonic Generation (THG, $\gamma^e(-3\omega;\omega,\omega,\omega)$), Electric Field Induced Second Harmonic (EFISH, $\gamma^e(-2\omega;\omega,\omega,0)$), Intensity-dependent Refractive Index (IDRI, $\gamma^e(-\omega;\omega,\omega,-\omega)$) and dc-Kerr Effect (dc-KE, $\gamma^e(0;\omega,-\omega,0)$).

According to the double harmonic oscillator approximation, vibrational contribution to polarizability was obtained through the following sum-over-modes expression [29]:

$$\alpha^v_{ij} = [\mu^2]^{0,0} = \sum_a^{3N-6} \frac{\left(\frac{\partial \mu_i}{\partial Q_a}\right)_0 \left(\frac{\partial \mu_j}{\partial Q_a}\right)_0}{\omega_a^2} \quad (1)$$

where ω_a is the circular vibrational frequency of the ath normal mode Q_a and $\partial\mu_i/\partial Q_a$ is the partial derivative of the i-component of μ with respect to Q_a. For second-order hyperpolarizability, we investigated IDRI NLO process that by adopting the infinite optical frequency approximation can be expressed as [30]:

$$\gamma^v_{ijkl}(-\omega_\sigma;\omega_1,\omega_2,\omega_3)_{\omega\to\infty} = \frac{2}{3}[\alpha^2]^{0,0} = \frac{2}{3}\times\frac{1}{8}\sum P_{-\sigma,1,2,3} \times \sum_a^{3N-6} \frac{\left(\frac{\partial \alpha_{ij}}{\partial Q_a}\right)_0 \left(\frac{\partial \alpha_{kl}}{\partial Q_a}\right)_0}{\omega_a^2} \quad (2)$$

where $\Sigma P_{\sigma,1,2,3}$ denotes the summation over the permutations of the $(-\omega_\sigma,i)$ $(\omega_1,j)(\omega_2,k)(\omega_3,l)$ pairs, and $\partial\alpha_{ij}/\partial Q_a$ is the polarizability derivative.Dipole moment and (hyper)polarizabilities are usually expressed as averaged values (μ, $<\alpha>$ and $<\gamma>$) and anisotropy of polarizability ($\Delta\alpha$):

$$\mu = \sqrt{\mu_x^2+\mu_y^2+\mu_z^2} \quad (3)$$

$$<\alpha> = \frac{1}{3}(\alpha_{xx}+\alpha_{yy}+\alpha_{zz}) \quad (4)$$

$$\Delta\alpha = \left\{\frac{1}{2}\left[(\alpha_{xx}-\alpha_{yy})^2+(\alpha_{xx}-\alpha_{zz})^2+(\alpha_{yy}-\alpha_{zz})^2\right]\right\} \quad (5)$$

$$<\gamma> = \frac{1}{5}\left[(\gamma_{xxxx}+\gamma_{yyyy}+\gamma_{zzzz})+2(\gamma_{xxyy}+\gamma_{xxzz}+\gamma_{yyzz})\right] \quad (6)$$

All calculations were performed with PC GAMESS [31,32] and Gaussian 03 packages [33].

3. Results and discussion

3.1. Geometry and torsional potential

Table 1 lists some selected geometrical parameters of NNs obtained at the B3LYP/cc-PVDZ level of calculation.

Table 1
Selected geometrical parameters of 1-nitronaphthalene, 2-nitronaphthalene and nitrobenzene

	1-NN	2-NN	NB	
	Calc.	Calc.	Calc.	Exp.[a]
C_1–C_2	1.381	1.377	1.395	1.399
C_2–C_3	1.410	1.415	1.396	1.386
C_3–C_4	1.378	1.376	1.400	1.399
C_4–C_{10}	1.421	1.425		
C_5–C_{10}	1.423	1.422		
C_5–C_6	1.376	1.379		
C_6–C_7	1.415	1.419		
C_7–C_8	1.380	1.378		
C_8–C_9	1.425	1.424		
C_1–C_9	1.435	1.419		
C_9–C_{10}	1.442	1.436		
C_1–N_{11}	1.482		1.480	1.486
C_2–N_{11}		1.478		
O_{12}–N_{11}	1.228	1.226	1.225	1.223
O_{13}–N_{11}	1.226	1.226		
C_1–N_{11}–O_{12}	118.6		117.5	117.3
C_1–N_{11}–O_{13}	117.3			
C_2–N_{11}–O_{12}		117.8		
C_2–N_{11}–O_{13}		117.3		
O_{12}–N_{11}–O_{13}	124.1	124.9	125.0	125.4
C_9–C_1–N_{11}	122.4		118.8	118.3
C_2–C_1–N_{11}	115.2			
C_1–C_2–N_{11}		118.8		
C_3–C_2–N_{11}		118.7		
C_1–C_2–C_3	120.4	122.5	118.5	117.6
C_2–C_3–C_4	119.7	118.7	120.2	120.6
C_3–C_4–C_{10}	121.2	121.3	120.3	120.2
C_1–C_9–C_8	125.8	121.8		
C_4–C_{10}–C_5	120.3	122.3		
C_9–C_1–N_{11}–O_{12}	24.0			
C_2–C_1–N_{11}–O_{12}	23.1			
C_1–C_2–N_{11}–O_{13}		0.0		
C_3–C_2–N_{11}–O_{13}		0.0		
C_1–C_9–C_{10}–C_5	179.0	180.0		
C_4–C_{10}–C_9–C_8	179.1	180.0		

Note that calculations are carried out at the B3LYP/cc-pVDZ level. Bond lengths in Å, bond angles in degrees, dihedral angles in degrees.
[a] Electron diffraction, Ref. [34].

For both isomers the computed structure is a stationary point in the potential energy surface (no imaginary vibrational wavenumbers). To the best of our knowledge, no experimental structures for NNs have been reported so far. B3LYP/cc-pVDZ geometrical parameters of NB, for which electron diffraction structure is available [34], are included in the Table. The overall agreement between optimized and experimentally determined structure of NB is satisfactorily. In addition, our results on NNs are in good agreement with those previously obtained by Onchoke et al. at the B3LYP/6-31G* level [7]. Present calculations show that 1-NN is characterized by O–N–C–C dihedral angles of 23° and 24°, owing to the steric hindrance effects between nitro group and hydrogen atom in position 8. On the other hand, 2-NN exhibits a planar arrangement and is more stable than 1-NN isomer by 4.1 kcal/mol at the B3LYP/cc-pVDZ level of theory, indicating stronger

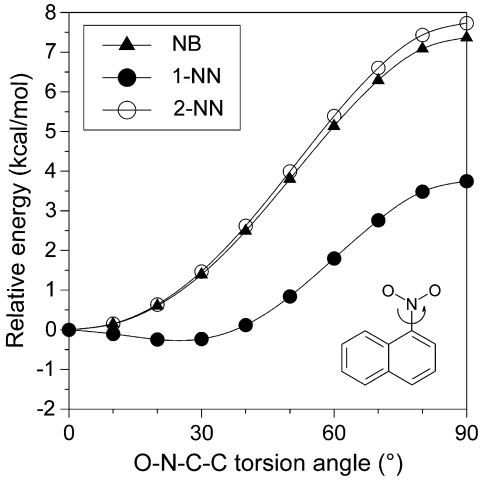

Fig. 2. Torsional potential of the investigated compounds.

π-conjugation effects. This is also reflected on the C–N bond length which shortens by 0.004 Å on going from 1-NN to 2-NN isomer. However, owing to the above steric effects, the largest deviation between NN isomers occurs for the C_9–C_{10} bond length, which elongates by 0.006 Å upon going from 2-NN to 1-NN. Note that naphthalene backbone is almost planar, the largest deviation for C–C–C–C dihedral angles being within 1°. Barrier heights for the internal rotation of the nitro group around the C–N bond were evaluated at the B3LYP/cc-pVDZ level of computation. The relaxed curves obtained in the 0°–90° range of the torsional angle in step of 10° are depicted in Fig. 2. The results show that 1-NN isomer exhibits two saddle-points with O–N–C–C dihedral angles of 0° and 90°. The corresponding barrier heights are computed to be 0.24 and 3.99 kcal/mol, respectively. Note that in the case of 2-NN isomer, $\Delta E_{0\rightarrow 90}$ value is calculated at 7.73 kcal/mol (which is somewhat similar to that obtained for NB at 7.36 kcal/mol) being about two times higher than that predicted for 1-NN isomer, indicating, consistently with a decrease of the C–N bond length, a stronger NO_2-ring π-conjugative interaction.

3.2. Dipole moments and electronic (hyper)polarizabilities

Calculations of electric properties were performed on the B3LYP/cc-pVDZ geometry. In order to evaluate the reliability of different levels of theory to determine μ^e, α^e and γ^e values, we first conducted calculation for NB for which both experimental [35–37] and theoretical data [38–40] are available from the literature. The calculated μ_i, $\alpha^e{}_{ii}$ and $\gamma^e{}_{iijj}$ components ($i, j = x, y, z$) for NB are collected in Table 2. As well established in the literature, introduction of diffuse functions as well as of electron correlation contributions are crucial for obtaining reliable values of electrical properties [41,42]. In fact on passing from 6-31G* to 6-31+G* $\langle\alpha^e\rangle$ and $\langle\gamma^e\rangle$ values increase by 16% and 240%, respectively, improving noticeably the

Table 2
Dipole moments, μ (Debye), static electronic polarizabilities, α^e (a.u.), and second hyperpolarizabilities, γ^e (a.u.), of nitrobenzene

	HF/6-31G*	HF/6-31+G*	HF/aug-cc-pVDZ	MP2/6-31+G*	PBE0/6-31+G*	Exp.
μ	5.24	5.35	5.15	4.49	4.90	4.22[a]
α^e_{xx}	85.6	93.0	96.0	95.1	94.2	
α^e_{yy}	93.9	101.6	107.8	107.8	111.0	
α^e_{zz}	26.2	44.4	49.7	45.1	44.2	
$\langle\alpha^e\rangle$	68.6	79.7[b]	84.5	82.7	83.1	87.0[c]
$\Delta\alpha^e$	64.0	53.4	53.2	57.4	60.2	
γ^e_{xxxx}	1285	6994	7523	8753	10,219	
γ^e_{yyyy}	16,894	26,603	26,311	42,903	42,140	
γ^e_{zzzz}	35	9775	8542	16,153	10,408	
γ^e_{xxyy}	−319	1191	1710	1516	2476	
γ^e_{xxzz}	67	4330	4164	8375	4908	
γ^e_{yyzz}	35	3032	3108	6465	3439	
$\langle\gamma^e\rangle$	3556	12,095[d]	12,068	20,104	16,883	17,075[e]

Note that calculations are carried out on the B3LYP/cc-pVDZ geometry.
[a] Gas phase value, from Ref. [35].
[b] $\langle\alpha^e\rangle(-\omega;\omega) = 80.0$ a.u., at $\hbar\omega = 0.02385$ a.u.
[c] DMSO solution, Ref. [36].
[d] $\langle\gamma^e\rangle(-3\omega;\omega,\omega,\omega) = 13{,}443$ a.u., at $\hbar\omega = 0.02385$ a.u.
[e] Liquid phase $\langle\gamma\rangle(-3\omega;\omega,\omega,\omega)$ value at $\hbar\omega = 0.02385$ a.u., Ref. [37].

agreement with experiment. Additionally, one notices that the properties obtained with 6-31+G* basis set reproduce satisfactorily those computed with the larger aug-cc-pVDZ basis set, with a difference of +3.9%, −5.7%, +0.4% and +0.2%, respectively, for μ, $\langle\alpha^e\rangle$, $\Delta\alpha^e$ and $\langle\gamma^e\rangle$. At the highest levels of computation, MP2/6-31+G* (PBE0/6-31+G*), the errors from experiment [35–37] for μ, $\langle\alpha^e\rangle$ and $\langle\gamma^e\rangle(-3\omega;\omega,\omega,\omega)$ [43] values are +6.4% (+13.9%), −4.9% (−4.5%) and +30.9% (+9.9%), respectively. The corresponding values for HF/6-31+G* level are +26.8%, −8.4% and −21.3%, respectively. It is worth to note that electric properties obtained by using PBE0 functional are in satisfactory agreement with MP2 data with a deviation of +9.1%, +0.5%, +4.9% and −16.0%, respectively, for μ, $\langle\alpha^e\rangle$, $\Delta\alpha^e$ and $\langle\gamma^e\rangle$ The above results allow us to conclude that, the PBE0/6-31+G* method can be a good compromise between accuracy and computational cost for the calculation of (hyper)polarizabilities of NNs.

Table 3 reports dipole moment and (hyper)polarizability values of NN isomers. For both NN isomers dipole moment vector is directed along the C–N bond axis. As previously found for NB, introduction of diffuse functions (6-31G* → 6-31+G*) as well as of electron correlation corrections (HF → PBE0) increase both $\langle\alpha^e\rangle$ and $\langle\gamma^e\rangle$ values. It is worth to mention that at the HF level of theory, on passing from 6-31+G* to aug-cc-pVDZ basis set μ and $\langle\gamma^e\rangle$ values decrease by 3.3–3.8% and 0.8%, respectively, while, $\langle\alpha^e\rangle$ and $\Delta\alpha^e$ values increase by

Table 3
Dipole moments, μ (Debye), static electronic polarizabilities, α^e (a.u.), and second hyperpolarizabilities, γ^e (a.u.), of 1-nitronaphthalene and 2-nitronaphthalene

	1-NN				2-NN			
	HF/6-31G*	HF/6-31+G*	HF/aug-cc-pVDZ	PBE0/6-31+G*	HF/6-31G*	HF/6-31+G*	HF/aug-cc-pVDZ	PBE0/6-31+G*
μ_x	−1.06	−1.06 (−1.14)	−1.04	−1.12	−5.39	−5.48	−5.30	−5.05
μ_y	−5.20	−5.32 (−5.45)	−5.12	−4.84	−2.38	−2.42	−2.35	−2.29
μ_z	−0.02	−0.02 (0.00)	−0.01	−0.02	0.00	0.00	0.00	0.00
μ	5.31	5.43 (5.57)	5.23	4.97	5.90	5.99	5.80	5.55
α^e_{xx}	161.9	173.5 (175.6)	179.2	180.7	178.0	190.6	199.0	208.2
α^e_{yy}	131.7	142.8 (144.1)	149.6	154.6	123.7	133.2	138.7	138.6
α^e_{zz}	40.3	67.5 (65.0)	73.4	66.7	37.9	64.9	71.3	64.2
$\langle\alpha^e\rangle$	111.3	127.9 (128.2)	134.1	133.9	113.2	129.6	136.3	137.0
$\Delta\alpha^e$	109.7	94.5 (98.7)	94.5	103.3	122.3	109.0	110.6	124.7
γ^e_{xxxx}	16,643	36,918 (36,660)	36,283	46,346	51,319	77,899	76,486	132,217
γ^e_{yyyy}	23,442	39,102 (42,364)	37,127	59,628	5649	15,058	14,688	20,632
γ^e_{zzzz}	54	13,884 (13,792)	12,689	14,738	45	13,673	12,153	14,534
γ^e_{xxyy}	−867	2515 (2726)	3569	9633	3541	7604	8332	16,845
γ^e_{xxzz}	104	8244 (8460)	8301	9253	120	6919	7126	7614
γ^e_{yyzz}	−17	5032 (4982)	5315	5866	66	5433	5579	6306
$\langle\gamma^e\rangle$	7672	24,297 (25,030)	24,094	34,043	12,893	29,308	29,080	45,783

Note that calculations are carried out on the B3LYP/cc-pVDZ geometry. Value in parentheses refers to the planar structure of 1-NN.

4.6–4.9% and 0.0–1.4%, respectively. The above results indicate that the larger basis set effects are mainly due to the contributions of the polarized and especially diffuse functions on the heavy atoms, confirming that 6-31+G* basis set is suitable for (hyper)polarizability computations, in agreement with present results on NB and the conclusions previously reported by Torrent-Sucarrat et al. [25]. At the PBE0/6-31+G* level of calculation, introduction of the benzene ring (NB → 2-NN) increases μ, $\langle\alpha^e\rangle$ and $\langle\gamma^e\rangle$ value by 13.3%, 64.9% and 171.2%, respectively. The results show that, for 1-NN isomer the largest (hyper)polarizability components are α^e_{xx} and γ^e_{yyyy}, which contribute to 45% and 27% of the total values, respectively. On the other hand, for 2-NN isomer both the longitudinal α^e_{xx} and γ^e_{xxxx} components exhibit the largest values, being 51% and 58% of the total values, respectively. At the highest level of calculation (PBE0/6-31+G*), on passing from 1-NN to 2-NN isomer μ, $\langle\alpha^e\rangle$, $\Delta\alpha^e$ and $\langle\gamma^e\rangle$ values increase by 11.7%, 2.3%, 20.7% and 34.5%, respectively, indicating stronger π-conjugation effects. Note that these differences are much more pronounced for the longitudinal components α^e_{xx} and γ^e_{xxxx}, which increase by 15.2% and 185.3%, respectively. However, it is worth to note that even if these increments are significantly influenced by the position of the substituent they are little dependent on the loss of co-planarity between the nitro group and the aromatic moiety. In fact, with reference to 1-NN isomer, on passing from the minimum-energy form to the planar structure, μ, $\langle\alpha^e\rangle$ and $\langle\gamma^e\rangle$ values increase by only 2.6%, 0.2% and 3.0%, respectively (See Table 3).

It is known that experimental EA and ionization potential values of NN isomers are close to each other [12,44], suggesting that oxidative and reductive mechanism arguments cannot be used to explain their different mutagenic behavior. Alternatively, the increase of mutagenic activity on passing from 1-NN to 2-NN isomer might be attributed to differences in substrate–enzyme binding affinity as determined by intermolecular interactions. This conclusion is supported by the above results obtained on all the electric properties. Additionally, our results and especially those on μ, $\Delta\alpha^e$, α^e_{xx} and γ^e_{xxxx}, are consistent with the conclusions previously traced by Yu et al. [45], for which mutagenic potency is maximized for isomers with the nitro substituent lying on the longest molecular axis. Recently, the different mutagenic behavior of 1-NN and 2-NN isomers has been elucidated on the basis of electron charge distributions described by IR and Raman intensities of vibrations mainly localized on the nitro group [46].

It is of interest to evaluate dynamic (hyper)polarizabilities, because experimental data are nearly always observed at incident optical fields. Frequency-dependent $\langle\alpha^e\rangle$ and $\langle\gamma^e\rangle$ values of NB and NNs obtained at the TD-HF/6-31+G* level of theory are summarized in Table 4. For all the compounds, as should be expected, the dynamic $\langle\gamma^e\rangle$ values occur according the order $\gamma^e(-3\omega;\omega,\omega,\omega) > \gamma^e(-2\omega;\omega,\omega,0) > \gamma^e(-\omega;\omega,\omega,-\omega) > \gamma^e(-\omega;\omega,0,0) > \gamma^e(-0;0,0,0)$. In the case of 2-NN isomer at $\hbar\omega = 0.04282$ a.u. ($\lambda = 1064$ nm), dispersion effects increase the static $\langle\alpha^e\rangle$ value by ca. 2%. For $\langle\gamma^e\rangle$, dispersion corrections to the static value obtained at $\hbar\omega = 0.02385$ a.u. ($\lambda = 1910$ nm) for the THG, EFISH, IDRI and dc-KE processes amount to 17%, 8%, 5% and 2%, respectively. At $\hbar\omega = 0.04282$ a.u. the percentages of increment are obviously higher, being 82%, 29%, 18% and 8%, respectively, the THG datum suffering of substantial resonant contributions. Comparable dispersion effects to $\langle\alpha^e\rangle$ and $\langle\gamma^e\rangle$ values are also found for 1-NN isomer. Note that dispersion effects for $\gamma^e(-3\omega;\omega,\omega,\omega)$ of NB, for which an experimental estimate at $\hbar\omega = 0.02385$ a.u. is available [37], are slightly lower (11%).

3.3. Vibrational (hyper)polarizabilities

Table 5 collects vibrational (hyper)polarizability values of the investigated compounds obtained through Eqs. (1) and (2) at the HF/6-31+G* level on the geometry optimized at the same level. As can be seen from the Table, $\langle\alpha^v\rangle$ values of NN isomers are almost close to each other, giving a modest but non negligible contribution to the total polarizability, the $\langle\alpha^v\rangle/\langle\alpha^e\rangle$ ratios being in the 0.07–0.08 range. For 1-NN the most important contributions come from low-frequency torsional modes. By contrast 2-NN, in analogy to NB, the largest contributions originate from intense IR absorptions located at higher energy values, attributed to the C–H out-of-plane bending and the symmetrical and asymmetrical stretching of the N–O bonds

Table 4
Frequency-dependent averaged electronic dipole polarizabilities $\langle\alpha^e\rangle(-\omega;\omega)$ (a.u.) and second hyperpolarizabilities $\langle\gamma^e\rangle(-\omega_\sigma;\omega_1,\omega_2,\omega_3)$ (a.u.) of nitrobenzene, 1-nitronaphthalene and 2-nitronaphthalene

	NB			1-NN			2-NN		
$\hbar\omega$ (a.u.)	0.02385	0.03457	0.04282	0.02385	0.03457	0.04282	0.02385	0.03457	0.04282
$\langle\alpha^e\rangle(0;0)$	79.6	79.6	79.6	127.9	127.9	127.9	129.6	129.6	129.6
$\langle\alpha^e\rangle(-\omega;\omega)$	80.0	80.3	80.7	128.6	129.3	130.1	130.2	131.0	131.8
$\langle\gamma^e\rangle(0;0,0,0)$	12,095	12,095	12,095	24,297	24,297	24,297	29,308	29,308	29,308
$\langle\gamma^e\rangle(0;\omega,-\omega,0)$	12,302	12,538	12,787	24,846	25,485	26,163	30,026	30,853	31,741
$\langle\gamma^e\rangle(-\omega;\omega,\omega,-\omega)$	12,516	13,014	13,562	25,422	26,793	28,366	30,778	32,567	34,614
$\langle\gamma^e\rangle(-2\omega;\omega,\omega,0)$	12,736	13,520	14,418	26,024	28,246	30,972	31,561	34,441	37,932
$\langle\gamma^e\rangle(-3\omega;\omega,\omega,\omega)$	13,443	15,295	17,779	28,025	33,884	44,016	34,151	41,540	53,256

Note that calculations are carried out at the HF/6-31+G* level on B3LYP/cc-pVDZ geometry.

Table 5
Main vibrational contributions and total vibrational (hyper)polarizabilities of nitrobenzene, 1-nitronaphthalene and 2-nitronaphthalene

	ω (cm^{-1})	I_{IR} (km/mol)	Mode[a]	$[\mu^2]$ (a.u.)	$\frac{<\alpha_v>}{<\alpha_e>}$	ω (cm^{-1})	A_{Raman} (Å^4/amu)	Mode[a]	$2/3[\alpha^2]$ (a.u.)	$\frac{<\gamma_v>}{<\gamma_e>}$[b]
NB	804	119	γ C–H	1.6		191	2	τ ring	496	
	1628	318	ν_s NO_2	1.1		1092	40	Ring br.	481	
	1841	389	ν_a NO_2	1.0		1628	96	ν_s NO_2	451	
			Total	6.6	0.08			Total	3267	0.24
1-NN	60	1	τ NO_2	1.1		60	2	τ NO_2	5586	
	109	1	τ ring	1.0		109	3	τ ring	2442	
	884	89	γ C–H	1.0		1469	295	ν ring	1803	
			Total	10.2	0.08			Total	15,006	0.53
2-NN	865	94	γ C–H	1.1		103	2	τ ring	1781	
	1631	241	ν_s NO_2	0.8		1496	318	ν ring	1784	
	1845	275	ν_a NO_2	0.7		1631	306	ν_s NO_2	1334	
			Total	9.4	0.07			Total	9973	0.29

Note that calculations are carried out at the HF/6-31+G* level on the HF/6-31+G* geometry.
[a] ν, stretching; γ, out-of-plane bending; τ, torsion; br., breathing.
[b] $<\gamma^v>(-\omega;\omega,\omega,-\omega)/<\gamma^e>(-\omega;\omega,\omega,-\omega)$ at $\hbar\omega = 0.04282$ a.u.

vibrations. Differently from $<\alpha^v>$, calculations indicate that $<\gamma^v>$ (2-NN) $<$ $<\gamma^v>$ (1-NN). Vibrational second hyperpolarizability values are predicted to be comparable to the electronic counterparts with $<\gamma^v>(-\omega;\omega,\omega,-\omega)/<\gamma^e>(-\omega;\omega,\omega,-\omega)$ ratios of 0.24, 0.53 and 0.29, for NB, 1-NN and 2-NN, respectively. The largest contributes principally come from low-frequency NO_2 group and ring torsional modes, as well as from high-frequency N–O bonds and ring stretching vibrations. It is worth to mention that, the difference in $<\gamma^v>$ value between 1-NN and 2-NN isomer is mainly ascribed to the remarkable contribution from the NO_2 torsion mode, which in the former isomer contribute to ca. 40% of the total $<\gamma^v>(-\omega;\omega,\omega,-\omega)$ value.

4. Conclusions

Dipole moment, static and frequency-dependent electronic and vibrational (hyper)polarizabilities of nitronaphthalene isomer were studied using ab initio and DFT-PBE0 methods in conjunction with 6-31G*, 6-31+G* and aug-cc-pVDZ basis sets. The obtained results indicate that all electric properties increase on passing from 1-NN to 2-NN isomer, consistently with the increase of π-conjugative interaction and the increase of the observed mutagenic activities. The increments of the electric properties are significant along the longitudinal axis but are little influenced by the loss of co-planarity between the nitro substituent and the aromatic ring system. These findings support the binding to enzyme through intermolecular interactions as an important step in the metabolic pathways for mutagenic activation of these nitroaromatic species.

Acknowledgements

This work was carried out in the framework of the RIC action of the Project No. 1999/IT.16.1.PO.011/3.13/7.2.4/339 PROT. 238, ''Formazione per la ricerca nel campo della bonifica dei siti contaminati'' POR Sicilia 2000–2006, Asse: III Misura: 3.13.

References

[1] H. Tokiwa, Y. Ohnishi, Crit. Rev. Toxicol. 17 (1986) 23.
[2] P.P. Fu, Drug. Metab. Rev. 22 (1990) 209.
[3] J.C. Spain, Ann. Rev. Microbiol. 49 (1995) 523.
[4] R. Friemann, M.M. Ivkovic-Jensen, D.J. Lessner, C.L. Yu, D.T. Gibson, R.E. Parales, H. Eklund, J. Mol. Biol. 348 (2005) 1139.
[5] N. Sera, K. Fukuhara, N. Miyata, H. Tokiwa, Mutat. Res. 349 (1996) 137.
[6] S.-T. Lin, Y.-F. Jih, P.P. Fu, J. Org. Chem. 61 (1996) 5271.
[7] K.K. Onchoke, C.M. Hadad, P.K. Dutta, Polycyclic Aromat. Compd. 24 (2004) 37.
[8] Y.S. Li, P.P. Fu, J.S. Church, J. Mol. Struct. 550–551 (2000) 217, and references therein.
[9] H.S. Rosenkranz, R. Mermelstein, Mutat. Res. 114 (1983) 217.
[10] H.S. Rosenkranz, R. Mermelstein, in: C.M. White (Ed.), Nitrated Polycyclic Aromatic Hydrocarbons, Huthig Heidelberg, 1985, pp. 267–297.
[11] A.K. Debnath, R.L. Lopez de Compadre, G. Debnath, A.J. Shusterman, C. Hansch, J. Med. Chem. 34 (1991) 786.
[12] T. Heinis, S. Chowdhury, P. Kebarle, Org. Mass Spectrom. 28 (1993) 358.
[13] J.D. McKinney, K.E. Gottschalk, L. Pedersen, J. Mol. Struct. (Theochem) 105 (1983) 427.
[14] E. Fraschini, L. Bonati, D. Pitea, J. Phys. Chem. 100 (1996) 10564.
[15] B.J. Mhin, J.E. Lee, W. Choi, J. Am. Chem. Soc. 124 (2002) 144.
[16] R.S. Asatryan, N.S. Mailyan, L. Khachatryan, B. Dellinger, Chemosphere 48 (2002) 227.
[17] S. Hirokawa, T. Imasaka, T. Imasaka, Chem. Res. Toxicol. 18 (2005) 232.
[18] V. Librando, A. Alparone, Environ. Sci. Technol. 41 (2007) 1646.
[19] C. Gu, X. Jiang, X. Ju, G. Yu, Y. Bian, Chemosphere 67 (2007) 1325.
[20] A.D. Becke, J. Chem. Phys. 98 (1993) 1372.
[21] C. Lee, A.D. Yang, R.G. Parr, Phys. Rev. B 37 (1988) 785.
[22] D.E. Woon, T.H. Dunning, J. Chem. Phys. 100 (1994) 2975.
[23] J.P. Perdew, K. Burke, M. Ernzerhof, Phys. Rev. Lett. 78 (1997) 1396.
[24] W.J. Hehre, L. Radom, P.v.R. Schleyer, J.A. Pople, Ab Initio Molecular Orbital Theory, John Wiley and Sons Inc, New York, 1986.
[25] M. Torrent-Sucarrat, M. Solà, M. Duran, J.M. Luis, B. Kirtman, J. Chem. Phys. 118 (2003) 711.

[26] H.A. Kurtz, J.J.P. Stewart, K.M. Dieter, J. Comput. Chem. 11 (1990) 82.
[27] S.P. Karna, M. Dupuis, J. Comput. Chem. 12 (1991) 487.
[28] H. Sekino, R.J. Bartlett, J. Chem. Phys. 85 (1986) 976.
[29] D.M. Bishop, Adv. Chem. Phys. 104 (1998) 1.
[30] D.M. Bishop, M. Hasan, B. Kirtman, J. Chem. Phys. 103 (1995) 4157.
[31] M.W. Schmidt, K.K. Baldridge, J.A. Boatz, S.T. Elbert, M.S. Gordon, J.H. Jensen, S. Koseki, N. Matsunaga, K.A. Nguyen, S.J. Su, T.L. Windus, M. Dupuis, J.A. Montgomery, J. Comput. Chem. 14 (1993) 1347.
[32] A.A. Granovsky, PC GAMESS version 7.0. Available from: <http://classic.chem.msu.su/gran/gamess/index.html/>.
[33] M.J. Frisch, G.W. Trucks, H.B. Schlegel, G.E. Scuseria, M.A. Robb, J.R. Cheeseman, V.G. Zakrzewski, J.A. Montgomery Jr., R.E. Stratmann, J.C. Burant, S.Dapprich, J.M. Millam,A.D.Daniels,K.N.Kudin,M.C. Strain,O. Farkas, J. Tomasi, V. Barone,M. Cossi, R. Cammi, B.Mennucci, C. Pomelli, C. Adamo, S. Clifford, J. Ochterski, G.A. Petersson, P.Y. Ayala, Q. Cui, K. Morokuma, D.K.Malick,A.D. Rabuck, K. Raghavachari, J. Cioslowski, J.V. Ortiz, A.G. Baboul, B.B. Stefanov, G. Liu, A. Liashenko, P. Piskorz, I. Komoromi, R. Gomperts, R.L. Martin, D.J. Fox, T. Keith, M.A. Al-Laham, C.Y. Peng, A. Nanayakkara, C. Gonzalez, M. Challacombe, P.M.W. Gill, B. Johnson, W. Chen, M.W. Wong, J.L. Andres, M. Head-Gordon, E.S., Replogle, J.A. Pople, GAUSSIAN-03, Rev. B.03 Gaussian Inc., Pittsburgh, PA, 2003.
[34] A. Domenicano, G. Schultz, I. Hargittai, M. Colapietro, G. Portalone, P. George, C.W. Bock, Struct. Chem. 1 (1989) 107.
[35] C.P. Smyth, Dielectric Behaviour and Structure, McGraw-Hill, New York, 1955.
[36] K.D. Singer, A.F. Garito, J. Chem. Phys. 75 (1981) 3572.
[37] L.-T. Cheng, W. Tam, S.H. Stevenson, G.R. Meredith, G. Rikken, S.R. Marder, J. Phys. Chem. 95 (1991) 10631.
[38] C. Daniel, M. Dupuis, Chem. Phys. Lett. 171 (1990) 209.
[39] N. Matsuzawa, D.A. Dixon, J. Phys. Chem. 98 (1994) 2545.
[40] R.H.C. Janssen, D.N. Theodorou, S. Raptis, M.G. Papadopoulos, J. Chem. Phys. 111 (1999) 9711.
[41] G.D. Purvis, R.J. Bartlett, Phys. Rev. A 23 (1981) 1594.
[42] J.E. Rice, R.D. Amos, S.M. Colwell, N.C. Handy, J. Sanz, J. Chem. Phys. 93 (1990) 8828.
[43] Note that correlated dynamic $\langle\gamma^{e}\rangle(-3\omega;\omega,\omega,\omega)$ values are here estimated by using HF dispersion ratios as commonly employed in the literature, $<\gamma^{e}>(-3\omega;\omega,\omega,\omega)_{corr} = \frac{<\gamma^{e}>(-3\omega;\omega,\omega,\omega)_{HF}}{<\gamma^{e}>(0;0,0,0)_{HF}} <\gamma^{e}> (0;0,0,0)_{corr}$, see for example T. Pluta, A.J. Sadlej, J. Chem. Phys. 114 (2001) 136.
[44] L. Klasinc, B. Kovac, H. Guesten, Pure Appl. Chem. 55 (1983) 289.
[45] S. Yu, D. Herreno-Saenz, D.W. Miller, R.H. Heflich, F.F. Kadlubar, P.P. Fu, Mutat. Res. 283 (1992) 45.
[46] V. Librando, A. Alparone, J. Hazard. Mater. (2008), doi:10.1016/j.jhazmat.2007.11.020.